Sensors and Actuators B 248 (2017) 622–629

Contents lists available at ScienceDirect

Sensors and Actuators B: Chemical

journal homepage: www.elsevier.com/locate/snb

Research Paper

A nanoporous gold-polypyrrole hybrid nanomaterial for actuation

Ke Wang[a,*], Charlotte Stenner[a], Jörg Weissmüller[a,b]

[a] Institute of Materials Physics and Technology, Hamburg University of Technology, Hamburg, Germany
[b] Institute of Materials Research, Materials Mechanics, Helmholtz-Zentrum Geesthacht, Geesthacht, Germany

ARTICLE INFO

Article history:
Received 26 October 2016
Received in revised form 17 March 2017
Accepted 5 April 2017
Available online 6 April 2017

Keywords:
Actuation
Hybrid
Nanoporous gold
Polypyrrole

ABSTRACT

We discuss actuation with a hybrid nanomaterial that is made by electro-polymerizing pyrrole on the internal surfaces of dealloying-derived nanoporous gold and then letting aqueous electrolyte be imbibed in the remaining pore space. In this way, active polypyrrole films are contacted by two separate but individually contiguous conduction paths, providing efficient transport of ions in the electrolyte channels and of electrons in the metal skeleton. The metal skeleton also serves to enhance the mechanical behavior of the actuator. Actuation exploits the dimension changes of the polymer when ions are exchanged with the electrolyte in a pseudo-capacitive way, at potentials negative of the classic oxidation/reduction of polypyrrole. Our experiments with millimeter-size bulk samples indicate fast switching and substantially larger strain amplitude than nanoporous metal actuators.

1. Introduction

Among materials for actuation, low-voltage electrochemical systems utilizing conducting polymers receive considerable attention [1,2]. The low voltage is safe, compatible with battery sources, and power input is potentially low [3]. Conducting polymers in contact with electrolyte can be oxidized or reduced by anodic or cathodic current. Ions and solvent are exchanged during these reaction, so that charge and osmotic pressure remain balanced. The composition variation is not only coupled to charge storage, but also to a volume change [4,5]. Thus, conducting polymer actuators exploit the coupling between the electric charge and mechanical strain during electrochemical processes that require low applied potentials [2,4,6,7]. As a drawback, rates of actuation tend to be low because of the relatively slow transport of ions within the polymer [6,8]. Thin film geometries, for instance in "ionic polymer metal composites" improve the kinetics, yet at the expense of large compliance [6]. Furthermore, the performance of conducting polymer actuators can be restricted by creep [3,9] and by the low stress that is sustained during actuation [3,10–12]. Here, we explore polypyrrole (PPy), a well investigated electroactive polymer system [13]. Exploiting a strategy that has been demonstrated for application as supercapacitors [14,15], we structure the PPy so that it contains separate conduction channels for ions as well electrons, interspersed at submicron scale. At the same time, we incorporate a mechanically robust metallic skeleton phase which enhances strength and stiffness.

Nanoporous metals made by dealloying [16–18] take the form of monolithic, millimeter sized bodies that consist of a homogenously interconnected network of nanoscale 'ligaments' and pore channels with a characteristic size that can be controlled down to well below 10 nm [19–21]. Nanoporous gold (NPG) provides a model system for dealloying-made metal nanostructures because of the material's particularly reproducible synthesis and its highly uniform microstructure. Due to size-effects, the ligaments that make up the metal skeleton are locally very strong. Thus, even though NPG is highly porous, significant values of the stiffness and of the effective macroscopic yield strength have been reported [22–26]. The mechanical performance is greatly enhanced when the pore space is filled with polymer, such as epoxy resin [27,28]. This observation suggests that NPG decorated with PPy as the active component might provide a hybrid nanomaterial that compromises between the large actuation amplitude of PPy and the good mechanical properties of metal nanomaterials.

Actuation is well documented for nanoporous metals with no PPy component [29–33]. When the pore space is filled with aqueous electrolyte, the materials actuate under electrochemical control of their surface stress [34,35]. This has been demonstrated for nanoporous gold [20,36], platinum [29,37], silver [32], nickel [33], palladium [38] and nanoporous Au-Pt alloy [21]. The materials are distinguished by their good electronic conductivity and by their strength and stiffness. On the other hand, strain amplitudes are considerably less than in polymer actuators and might benefit from enhancement.

* Corresponding author.
E-mail address: k.wang@tu-harburg.de (K. Wang).

http://dx.doi.org/10.1016/j.snb.2017.04.025

Hybrid materials made from NPG and conducting polymer have already been demonstrated in the contexts of charge storage and sensing. Meng et al.[14] explored thin films of PPy-decorated NPG as electrochemical supercapacitors with high power and energy density. In the same context, Lang et al. [15] investigated NPG-polyaniline hybrid films. Xiao et al.[39] reported a hybrid film made by electropolymerizing 3,4-ethylenedioxythiophene on NPG for applications as biosensors. Detsi et al.[40] presented a electrolyte-free actuation in a NPG-polyaniline hybrid material, again in thin-film form, emphasizing the high actuation strain rate of the material.

Here, we explore the NPG-polypyrrole system for actuation, with a specific focus on making not thin films but macroscopic, monolithic actuator materials. We show that by functionalizing the gold-electrolyte interface with thin PPy layers the actuation amplitude of the material can be strongly enhanced compared to actuation with pure NPG. At the same time, switching response times are found substantially faster than in bulk actuators from conductive polymers without the interpenetrating metal skeleton.

2. Material and methods

Cylindrically shaped NPG samples with diameter 0.9 mm and length of 1.5 mm were prepared by following the procedures in Ref. [28]. The $Au_{25}Ag_{75}$ master alloy was prepared by arc-melting, homogenized by annealing for 100 h at 850 °C, shaped to a cylinder by wire drawing and finally annealed in vacuum during 3 h at 650 °C for recovery.

The master alloy samples were dealloyed in 1 M $HClO_4$ prepared from $HClO_4$ (Suprapur R, Merck) and ultrapure water (18.2 MΩ cm) at dealloying potential 0.75 V and ambient temperature. When the current fell to below 10 μA, the potential was stepped to 0.85 V and held for 3 h, which completed the dealloying. In order to remove surface and subsurface oxides, the samples were then subjected to 40 potential cycles in the interval 0–1.0 V at scan rate of 10 mVs^{-1} [20]. Immersion in ultrapure water and drying in vacuum for 3 days followed. All samples were then annealed at 300 °C in air for 1 h to increase the ligament size. Energy dispersive x-ray spectroscopy in the scanning electron microscope (SEM) suggests that the resulting nanoporous material is essentially pure Au, with a residual Ag content of ≤2 at.-% [27].

With the exception of the electropolymerization (see below), all electrochemical experiments in this work used Ag/AgCl pseudo-reference electrodes, and all respective potentials are specified versus this electrode. The reference potential was measured as +0.202 V vs. versus an Ag/AgCl electrode in saturated KCl solution (World Precision Instruments, Inc., which is itself +200 mV vs. the standard hydrogen electrode, SHE). Thus, our potentials are shifted by +0.402 V versus SHE.

Bulk samples of nanoporous gold-polypyrrole (NPG-PPy) hybrid material were made by electrochemical polymerization of pyrrole in NPG. The commercial pyrrole monomer (Sigma-Aldrich) was purified by passing through a column of basic alumina and stored in a dark bottle at 4 °C. Commercial anhydrous $LiClO_4$ (Merck) and HPLC grade acetonitrile (Sigma-Aldrich) was used as received. The electrolyte solution was 0.1 M pyrrole and 0.1 M $LiClO_4$ in acetonitrile containing 2% water. In a three-electrode setup a Pt wire served as counter electrode and a saturated calomel electrode (SCE, World Precision Instruments) as reference electrode. Bulk NPG samples were used as the working electrode and firstly immersed into the electrolyte solution for ½ h. The polymerization of pyrrole to PPy used consecutive square waves of potential between −500 mV (2 s) and +800 mV (8 s) for 450, 900 and 2200 cycles, which needed in total around 1.25, 2.5 and 6 h, respectively. The hybrid material were then rinsed thoroughly with ultrapure water.

The electrochemical behavior of the hybrid material was characterized in 1 M $HClO_4$ aqueous electrolyte by three-electrode cyclic voltammetry at scan rates of 10 mV s^{-1}. Actuation measurements, also in 1 M $HClO_4$, used an *in-situ*, electrochemical cell inserted in a dynamic mechanical analyzer (DMA; BOSE ElectroForce), in combination with a potentiostat (Autolab). Fig. 1 illustrates the setup. Prior to all measurements the glassware was cleaned in Piranha solution and rinsed with ultrapure water. Carbon cloth served as counter electrode.

A scanning electron microscope (SEM; LEO 1530 Gemini) operated at 10 kV was used for characterization of microstructure and composition. Compression tests used a Zwick 1484 testing machine with the elongation measured between the load surfaces. A feedback loop controlled and progressively reduced the crosshead speed so as to maintain constant true strain rate at 10^{-4} s^{-1} while the sample length varied.

3. Results

3.1. Microstructure

SEM images prior to polymer decoration (Fig. 2A) illustrate the bicontinuous structure of NPG and the ligament size in our samples, $L = 250 \pm 50$ nm. In this first study we selected the comparatively large L in order to assure sufficient transport channel cross-section for easy monomer transport during polymerization and for fast ion transport during actuation.

The success of electrochemical polymerization of pyrrole is demonstrated in Fig. 2(B), which shows the fracture cross-section SEM micrograph of NPG-PPy hybrid material. A conformal coating of the ligaments with PPy, 80 nm thick, is apparent. The electropolymerization exploits the good adsorption of pyrrole monomers on gold surfaces and the high electrical conductivity of NPG electrodes [14]. The homogeneous PPy layer thickness, throughout the bulk nanoporous sample, suggests that attachment kinetics may limit the growth rate. The thickness of PPy layer for NPG-PPy hybrid nanomaterial can be tuned by adjusting the time, t_P, of the potentiodynamic polymerization. Hybrid nanomaterial with PPy layers of thickness 15 ± 5 nm (t_P = 1.25 h), 50 ± 10 nm (2.5 h) and 80 ± 20 nm (6 h) are shown in Fig. 2(C)–(E), respectively.

3.2. Electrochemical characterization

Fig. 3 summarizes electrochemical properties of pure NPG and NPG-PPy composite characterized by cyclic voltammograms in 1 M $HClO_4$. The dashed graphs in part (A) of the figure refer to pure NPG; note the distinct oxygen adsorption and desorption peaks with their onsets at around 0.8 V. The oxygen-on-gold electrosorption features are missing in the CVs of the NPG-PPy hybrid nanomaterial (solid lines). This shows that the gold surface is indeed completely coated by PPy. The prevailing feature of the CVs on the hybrid nanomaterials is an apparent adsorption peak with an onset at 0.91 V, and a corresponding desorption peak that is shifted substantially to negative potentials, with an onset at 0.75 V. This behavior is similar to earlier reports on voltammetry for PPy [41]. A shift of the electrosorption peak in our scans to positive potential, as compared to published data, may be rationalized as the consequence of the pH-dependent potential [42] along with the acidic nature (pH ~ 1) of our electrolyte. The figure shows that repeated cycling to an upper potential vertex of 1.2 V leads to a slight decrease of the PPy-related peaks, while no oxygen-on-gold electrosorption feature appears.

Part B of Fig. 3 shows CVs in a larger potential interval. As the most obvious feature, the current increases drastically at the upper end of the potential scale, and the voltammogram degrades severely during the 10 cycles of the figure. Most remarkably, the

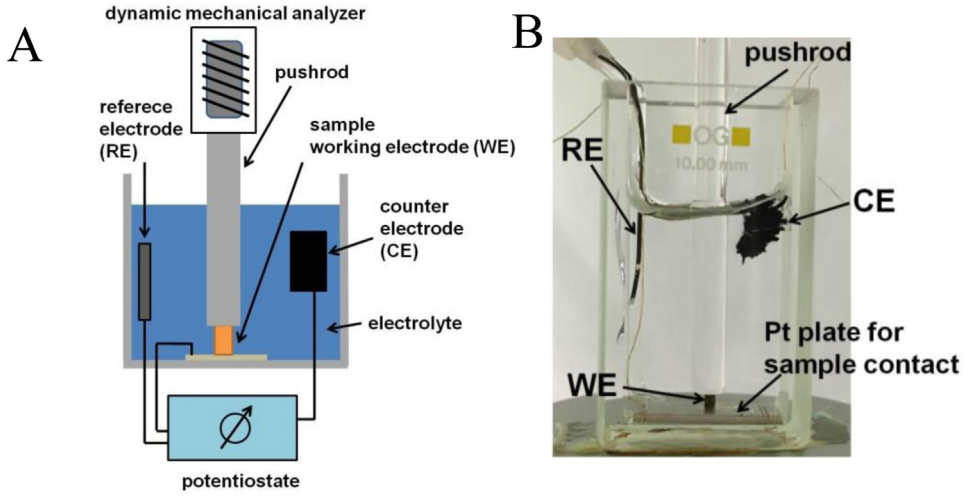

Fig. 1. (A) Schematic illustration of actuation measurements performed in situ in electrochemical cell arranged in dynamic mechanical analyzer (DMA) combined with potentiostat. (B) Photograph of electrochemical cell mounted in DMA. Glass cuvette served as in situ electrochemical cell and fused silica pushrod transfers load to the sample. RE, CE, and WE denote reference, counter, and working electrode, respectively.

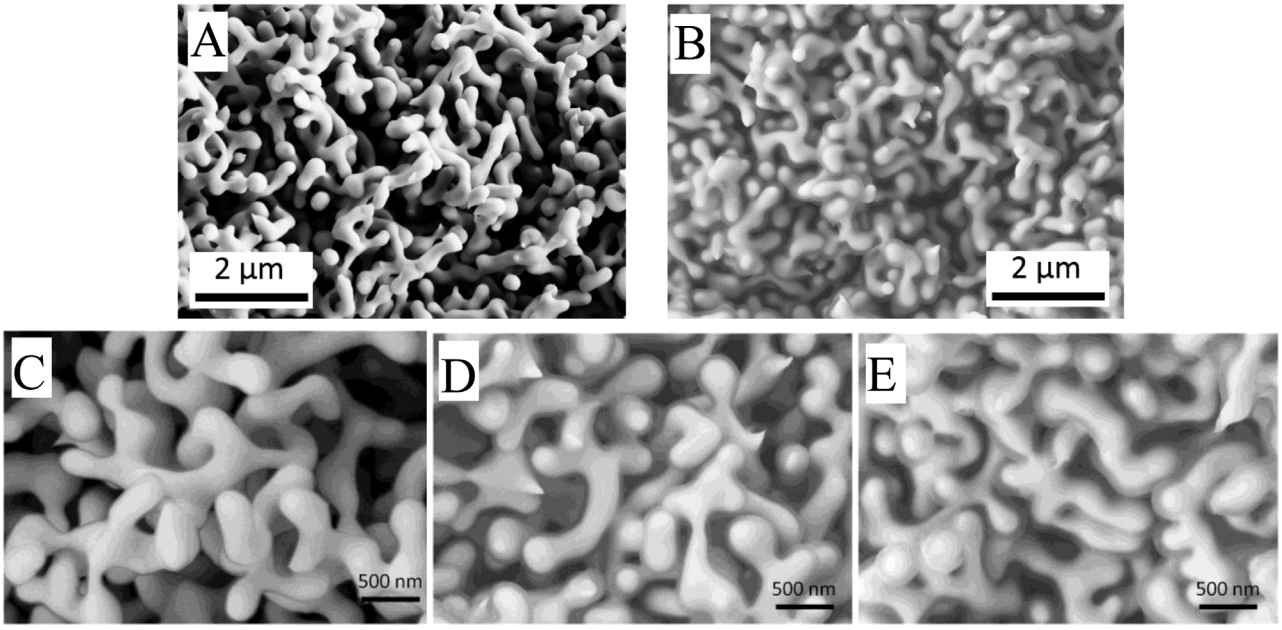

Fig. 2. (A) Scanning electron micrographs of bicontinuous open porosity of NPG with ligament diameter of about 250 ± 50 nm. (B) Scanning electron micrographs of cross-sectional surfaces of NPG-PPy composites, which clearly shows a conformal coating of PPy. It demonstrates that the electropolymerization is successful. Note that the water channel still remains. Large magnification SEM images of NPG-PPy composites with an approximate average PPy thickness of (C) 15 ± 5 nm, (D) 50 ± 10 nm and (E) 80 ± 20 nm, which is synthesized by electropolymerization for around 1.25 h, 2.5 h and 6 h.

final cycle appears consistent with the CV of gold in Fig. 3(A). This suggests that scans to >1.2 V lead to the removal of the PPy layer. This is consistent with reports of overoxidation of PPy at high potential [43–45]. The feature near the lower potential vertex (see inset in Fig. 3(B)) indicates an irreversible reaction that restricts the potential range at this end of the voltammogram.

Fig. 3(C) shows CVs in a smaller potential interval that avoids all electrosorption peaks and irreversible features, −0.1–0.4 V. In this regime the processes on pure NPG (black line) are essentially capacitive. In the hybrid samples, the charging/discharging currents increase with the layer thickness. Indeed, the graph of (pseudo-) capacitance, C, versus PPy layer thickness in Fig. 3(D) is highly linear. The substantially larger C of the NPG-PPy hybrid nanomaterials confirms the already established fact [14,15] that much larger amounts of charge can be stored in a pseudo-capacitive way in the hybrid material. We also found that CVs where highly reproducible over many potential cycles in this potential interval, indicating a good stability of the PPy layer.

3.3. Actuation

We first inspect actuation experiments which were performed, for the same NPG-PPy sample (50 nm layer thickness), in two different potential ranges: −0.1 to 0.4 V and 0.5–1 V. The scan rate was 2 mV s^{-1}. We measure the deformation during actuation by a macroscopic effective strain, ε, which is defined as the relative change in sample length, l. That is, we take $\varepsilon = \delta l/l_0$ with l_0 the initial length. In each actuation experiment, ε was measured during 8 subsequent potential scans. The representative results were shown in Fig. 4(A) and (B). It is seen that the sample expands with

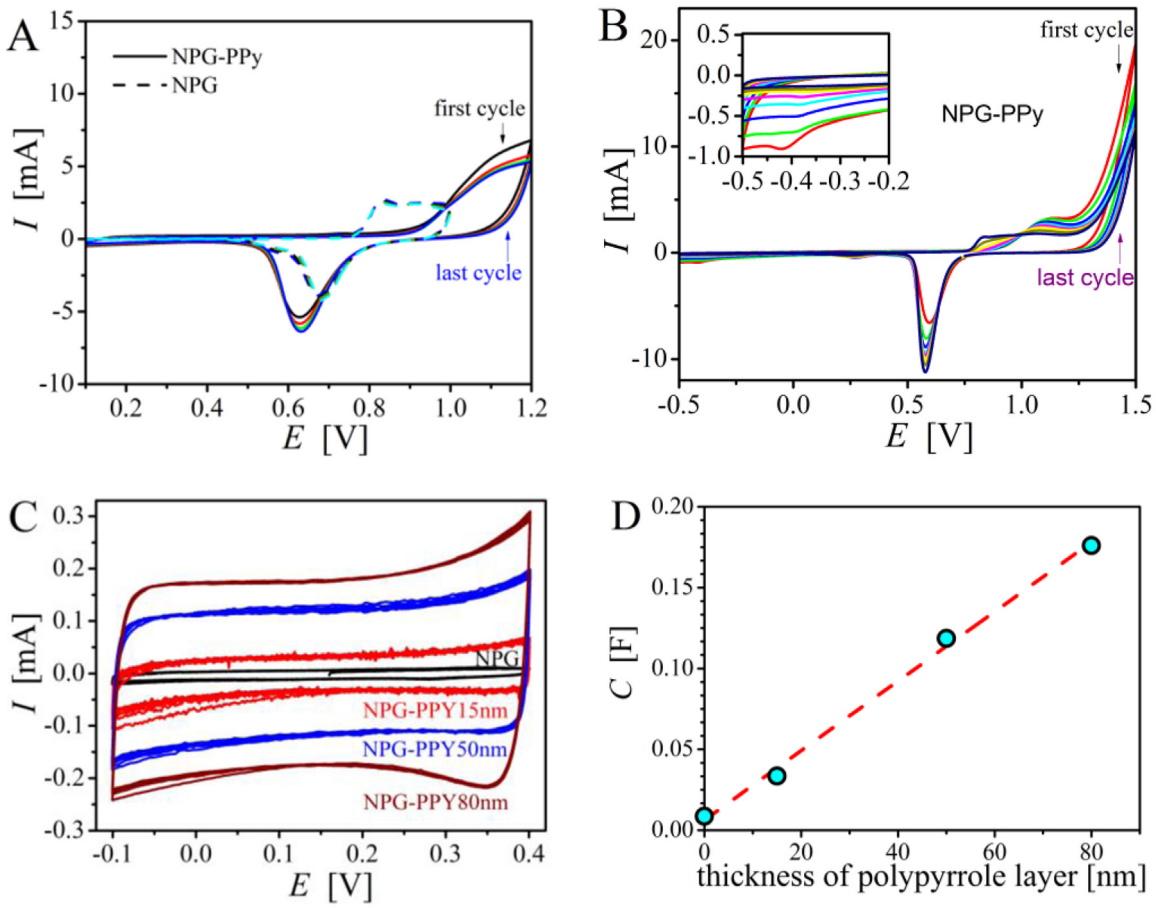

Fig. 3. Electrochemical characterization represented by cyclic voltammograms (CVs) of current I versus electrode potential E in 1 M $HClO_4$. (A) Five successive cyclic scans between −0.25 V and 1 V for nanoporous gold (dashed line) and between 0.1 and 1.2 V for NPG-PPy composite (solid line) at scan rate of 10 mV s^{-1}. (B) Ten successive cyclic scans between −0.25 and 1.5 V for NPG-PPy composite at scan rate of 10 mV s^{-1}. (C) Eight successive CV scans between −0.1 to 0.4 V at 2 mV s^{-1} for pure NPG and NPG-PPy composites with different thickness of PPy. (D) Pseudocapacitance, C, versus PPy layer thickness for all graphs of (C). The C was calculated from the average of the absolute current divided by scan rate.

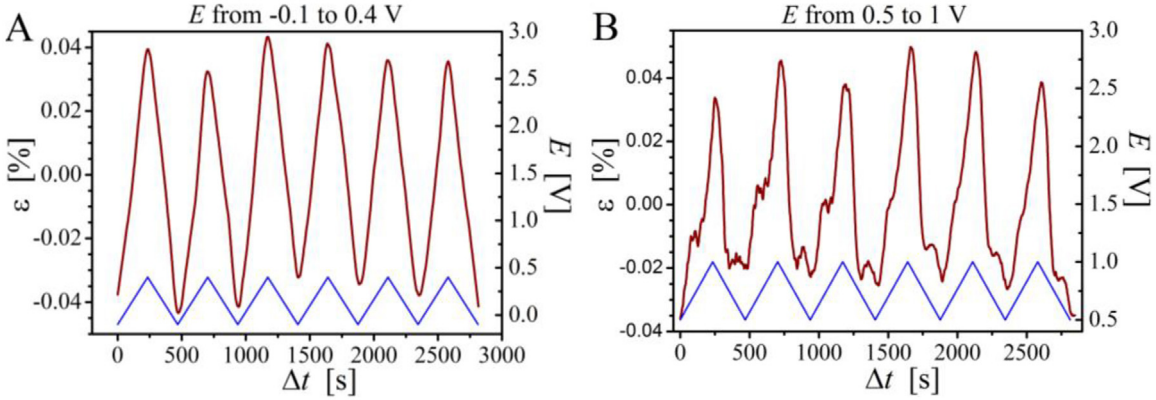

Fig. 4. Actuation measurements for NPG-PPy composite with PPy layer of 50 nm in 1 M $HClO_4$ at scan rate of 2 mV s^{-1} and in two different potential ranges: (A) −0.1 to 0.4 V and (B) 0.5–1 V. Six sweeps of potential, E, (blue line, right ordinate) versus time, Δt, are shown exemplarily. Strain, ε, (dark red line, left ordinate) increases with increasing E. (For interpretation of the references to colour in this figure legend, the reader is referred to the web version of this article.)

increasing potential. The mean peak-to-peak amplitudes, 0.075% and 0.073%, respectively, are nearly the same for the more negative and more positive potential intervals. Thus, the actuation in the potential regime −0.1 to 0.4 V achieves the identical strain as in the higher potential regime, but with less charge transport and less hysteresis. Therefore, all further investigations focused on −0.1 to 0.4 V potential interval.

Fig. 5 explores the actuation of samples with different PPy layer thickness. Transients of strain and potential (range −0.1 to 0.4 V, scan rate 2 mV s^{-1}) are shown in part (A). All PPy- covered samples expand during positive-going scans, consistent with swelling due to the uptake of anions. Fig. 5(B) shows the peak-to-peak actuation amplitude versus the PPy layer thickness. Similar to the capacity, the strain amplitude increases linearly with the layer thickness. The

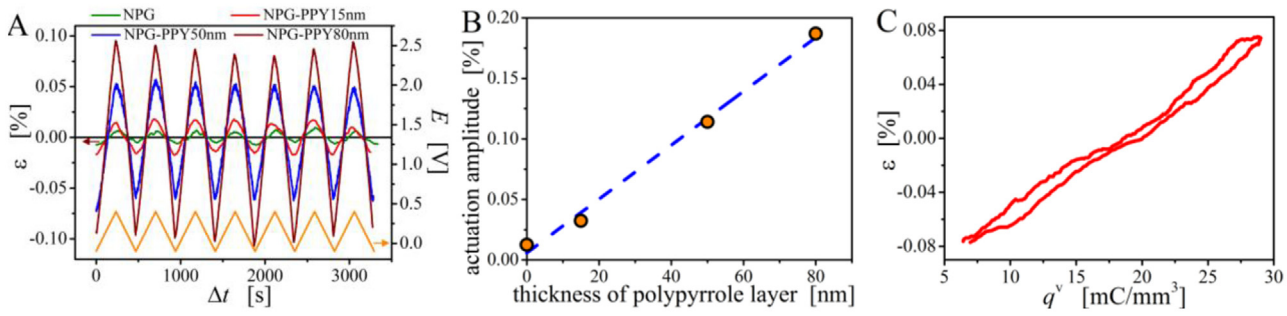

Fig. 5. Actuation measurements in 1 M $HClO_4$. (A) Mechanical characterization recorded simultaneously with cyclic voltamograms shown in Fig. 3(C): variation of potential, E, (right ordinate) with time, Δt, indicated by green line and corresponding values of effective strain, ε (left ordinate) indicated by blank, red, blue and dark red line for pure nanoporous gold, and NPG-PPy composite with PPy layer of 15 nm, 50 nm and 80 nm, respectively. (B) Actuation amplitude versus PPy layer thickness for the data in (A). These emphasize the enhancement of the properties over NPG. (C) Effective strain ε versus volume-specific charge, q^v, corresponding to the measurement shown in (A) for NPG-PPy with PPy thickness of 80 nm. Data was averaged over 3 actuation cycles, separately for positive and negative going sweeps. We can see reversible macroscopic strain in response to variation of volume-specific charge. (For interpretation of the references to colour in this figure legend, the reader is referred to the web version of this article.)

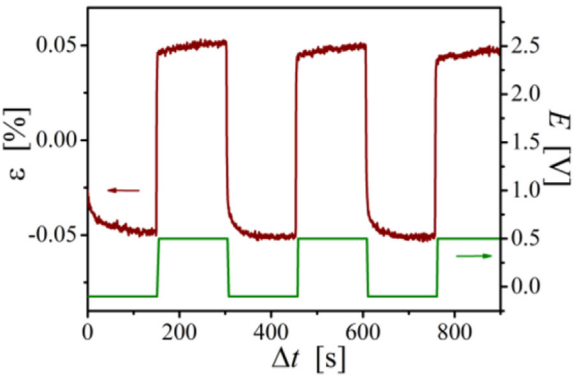

Fig. 6. Actuation measurements for NPG-PPy composite with PPy thickness of 50 nm in 1 M $HClO_4$ responds to step change of potential between −0.1 V and 5 V. Variation of potential E (right ordinate) with time, Δt, is indicated by green line and corresponding change of effective strain, ε (left ordinate) with time is indicated by dark red line. (For interpretation of the references to colour in this figure legend, the reader is referred to the web version of this article.)

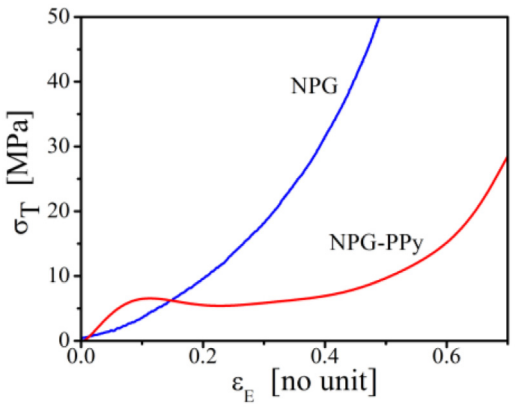

Fig. 7. Variation of true stress, σ_T, with engineering strain, ε_E, in compression tests with pure nanoporous gold (NPG) and in a nanomaterials from NPG and polypyrrole (PPy). Ligament sizes in both samples are 250 nm, PPy layer thickness is 50 nm.

strain amplitude, ~0.19%, of the 80 nm PPy layer sample is more than 12 times higher than the ~0.015% of pure NPG.

It is of interest to quantify the actuation behavior in terms of the charge-response of a measure for deformation. Proposed response coefficients can be specific for a device configuration – such as bimorph cantilevers [4] – or they can be materials-specific [46,47]. Since the deformation of our material may be assumed uniform in a coarse-grained picture that ignores the nanoscale microstructure, the experiments afford a direct characterization of the materials behavior. In their phenomenological thermodynamics analysis of actuation and sensing with hybrid nanomaterials, Stenner et al.[47] have defined an effective strain-charge coefficient, $A^* = {\rm d}\varepsilon/{\rm d}q^{\rm v}|_T$, as the response of the effective macroscopic strain ε to changes of the volume-specific charge, $q^{\rm v}$, measured at constant load T. Here, q^V is defined as net electric charge, Q, over total sample volume, V (solid and pores), with V measured in the strain-free reference state. Via A^* one can assess the induced strain per charge, standardized to the sample volume, and therefore quantitatively evaluate a material-specific actuation ability. Fig. 5B shows the averaged strain plotted versus $q^{\rm v}$ for the NPG-PPy sample with PPy thickness of 80 nm. The data was averaged from 3 actuation cycles, separately for positive and negative going sweeps. Linear regression provides $A^* = 0.0675 \pm 0.0004\ {\rm mm^3\ C^{-1}}$.

The actuation response rate may be parameterized by the time, $t_{½}$, required to reach half of the saturation strain after a potential jump. Fig. 6 shows results for jumps between −0.1 V and 0.5 V. For the example of the 50 nm layer thickness sample we find $t_{½} \approx 1$ s for both, expansion and contraction reactions.

3.4. Compression tests

Fig. 7 shows compressive stress-strain curves for mm-sized samples of NPG and NPG-PPy hybrid material with PPy layer thickness 50 nm and ligament size 250 nm. Excellent deformability was found for both materials. Upon loading, NPG exhibits an immediate yield onset with no elastic regime and a stress-strain graph with ever increasing work hardening. This agrees with previous results in Ref. [28,48]. As compared with the pure NPG, the NPG-PPy hybrid material samples present a substantially different stress-strain behavior. An initial elastic regime is more clearly expressed, even though the slope indicates a low Young's modulus, about 0.1 GPa. Yielding sets in at around 6 MPa; it is followed by a short plateau of constant flow stress and finally again a regime of strong work hardening.

4. Discussion

The discussion of our observation starts out with remarks on the actuation mechanism. For reference we first focus on NPG, a metallic structure without PPy coating and in contact with aqueous electrolyte. Here, polarizing the electrode surfaces impacts the interatomic bond forces between the metal atoms in the outermost interatomic plane [49,50]. In order to preserve the mechanical

equilibrium these changes in the surface stress are compensated by opposite changes in bulk stresses of the ligaments, resulting in overall macroscopic dimensional changes. The mechanics of actuation in the hybrid material with its PPy covered surfaces may be understood quite similarly. Here, potential variation results in a change in ion content in PPy layer. The layer can partly accommodate the resulting volume change by expanding freely in the direction normal to the Au-PPy interface. However, the layer is clamped in the in-plane directions. Its tendency for expansion here creates tangential stresses of opposite sign in the polymer and in the metal. The stresses in the metal translate into an overall expansion of the gold skeleton and, thereby, of the entire sample.

The nature of the ion exchange and the magnitude of the volume change of PPy depends on synthesis condition and on the electrolyte used for actuation. Smela et al. [2] emphasized that changing the synthesis conditions, such as the anion, solvent, or current density, yields what are essentially different materials. PPy is polymerized in the fully oxidized state, which has one positive charge along the backbone for every three to four pyrrole monomer units and an equal number dopant anions. The nature of the dopant impacts the properties of the polymer [13]. In our work, the PPy(ClO_4^-) system was chosen during polymerization because this system shows comparatively large actuation strain, see Fig. 8 in Ref. [51]. The electrolyte in our actuation experiment used the same anion, so that volume changes connect to the exchange of ClO_4^- [52].

While the above behavior is well-established, the potential range in which it is exploited in our experiment is not. Studies of both, ion exchange and actuation with PPy focus, to the best of our knowledge, invariably on the "oxidation/reduction" process that can be associated with the pronounced electrosorption peaks in cyclic voltammograms; our Fig. 3A displays these peaks in good agreement with the literature. Yet, our investigation of actuation points towards a range of more negative potentials, in which the CVs exhibit a smaller and nearly constant current, see Fig. 3C. The electrochemical signature is here phenomenologically similar to the capacitive regime of idealized metal electrodes.

Our results characterize the above, pseudo-capacitive regime as most appropriate for actuation because of its lack of hysteresis and the higher cycle stability. It is particularly remarkable that the strain per charge in our hybrid material is larger for pseudo-capacitive charging as compared to what we find in the classic oxidation/reduction regime. Furthermore, the apparent capacity and the actuation amplitude vary linearly with the PPy layer thickness in this regime. Obviously, pseudo-capacitive charging involves the exchange of anions between the aqueous medium and the PPy. Yet, the linear charge-potential relation as opposed to the electrosorption peak of the oxidation reduction reaction suggests a nonspecific interaction of the anions with the polymer. Pseudo-capacitive charging of PPy may then arise from the buildup of a space-charge layer, similar to the diffuse layer at a charged metal electrode surface. The screening of electric fields by space charge implies that such layers can only be observed in the immediate vicinity of a surface. The phenomenon would then be specific to thin PPy layers, such as those coating our nanoporous electrode.

Martinez et al. [53,54] investigated actuation in a geometry somewhat similar to ours, yet with much larger dimensions. Gold or Platinum wires, 500 μm in diameter, were coated with several μm thick PPy layers and the thickness variation of the PPy – i.e., the *radial* strain of the coated wire – during electrochemical cycles studied. Focusing on the oxidation/reduction process, this work found a linear charge-strain correlation, as in the present study. While Martinez et al. advertise substantial parasitic loss currents in their Au/PPy experiments, the data of our Figs. 3 and 5 C testify to an almost ideal pseudo-capacitive behavior, in which charge is practically completely recovered after potential cycles. Furthermore, the electrode potentials of the redox reaction differs between our work and Refs. [53,54]. The difference may be attributed to the different pH values of the electrolytes. On a more fundamental level, our approach differs from Martinez et al. in as much as the larger surface-to-volume ratio of our material affords coupling the deformation of the PPy into a *longitudinal* strain of the underlying metal. This is advantageous since the stiff metal skeleton here transmits the actuation effect to the external surface of the actuation body, where it can do work against external forces.

Regarding the actuation performance of our material, we emphasize that the switching response times of the bulk NPG-PPy hybrid materials are found substantially faster than in bulk actuators from conductive polymers without the interpenetrating metal skeleton. Early work on PPy actuators showed large strain, but long response times. For PPy films, Bay et al.[55] reported an actuation strain rate near 0.06%/s while Spinks et al.[56] found 0.01%/s. Even though our NPG-PPy hybrid material was investigated in the form of bulk samples of millimeter dimension, its strain rate of 0.1%/s exceeds those earlier values.

Besides revealing a ductile-brittle transition when going from the reduced to the oxidized state, in situ mechanical tests on PPy films indicate yield stresses around 3–5 MPa [57]. Compression tests on our NPG-PPy suggest similar yield strength, around 6 MPa, and extended deformability in compression.

In relation to the mechanical performance it is significant that our first exploration of the hybrid nanomaterials worked with comparatively large ligament size, $L = 250$ nm. The strength of bulk samples of NPG has been shown to vary as the inverse of L, down to ligament sizes tenfold less than those of the present samples [26]. Furthermore, the effective Young's modulus of NPG increases tenfold when going from $L = 150$ nm to 20 nm [26]. Thus, reducing L provides opportunities for substantially enhancing strength and stiffness of our material in future experiments. Studies of this effect are in preparation in our laboratory. Reducing L also has important repercussions for the actuation behavior that will require exploration. The PPy layers will need to be thinner, which reduces the anion exchange per internal surface area. On the other hand, the net surface area increases as $1/L$. The maximum total amount of PPy that can be accommodated in the hybrid material scales with the pore volume of the NPG matrix; this volume remains invariant during the downscaling of L. Thus, it may be expected that the overall actuation amplitude will be maintained at smaller ligament size, whereas strength and stiffness are expected to increase substantially.

5. Conclusions

We have explored an electrically tunable nanoporous gold based hybrid nanomaterial for actuation. In our actuation concept, a nanoscale him coating of polypyrrole is grown onto the internal metal surfaces by electrochemical polymerization, and the remaining pore space filled with aqueous electrolyte. In this way, the active polymer films are contacted by two separate but individually contiguous conduction paths, providing efficient transport of ions in the electrolyte channels and of electrons in the metal skeleton. The metal skeleton also carries load and thus defines the mechanical behavior of the actuator.

Contrary to earlier studies, our actuation does not exploit the classic oxidation/reduction of polypyrrole, but instead the exchange of anions with the polymer at more negative potentials. The exchange appears to involve the buildup of a space charge layer through unspecific ion accommodation within the polypyrrole layer. We find this process to provide somewhat larger actuation per charge transfer along with a better stability of the polymer.

The linear strain amplitude of our material reaches 0.19%, which is 12 times higher than that of pure nanoporous gold under similar conditions. Furthermore, switching times are attractive in view of the macroscopic dimensions of our actuators. The large strain amplitude, fast switching, and the availability of centimeter size monolithic samples distinguish the material as an actuator.

Acknowledgment

This work was funded by DFG through SFB 986 "Tailor-Made Multi-Scale Materials Systems – M^3", sub-project B2.

References

[1] T.F. Otero, J.M. Sansinena, Artificial Muscles Based on Conducting Polymers, Bioelectrochem. Bioenergy 38 (1995) 411–414.
[2] E. Smela, Conjugated polymer actuators for biomedical applications, Adv. Mater. 15 (2003) 481–494.
[3] G.M. Spinks, V. Mottaghitalab, M. Bahrami-Saniani, P.G. Whitten, G.G. Wallace, Carbon-nanotube-reinforced polyaniline fibers for high-strength artificial muscles, Adv. Mater. 18 (2006) 637–640.
[4] T.F. Otero, J.G. Martinez, J. Arias-Pardilla, Biomimetic electrochemistry from conducting polymers. A review: artificial muscles, smart membranes, smart drug delivery and computer/neuron interfaces, Electrochim. Acta 84 (2012) 112–128.
[5] T.F. Otero, Biomimetic conducting polymers: synthesis, materials, properties, functions, and devices, Polym. Rev. 53 (2013) 311–351.
[6] T. Mirfakhrai, J.D.W. Madden, R.H. Baughman, Polymer artificial muscles, Mater. Today 10 (2007) 30–38.
[7] T.F. Otero, Coulovoltammetric and dynamovoltammetric responses from conducting polymers and bilayer muscles as tools to identify reaction-driven structural changes. a review, Electrochim. Acta 212 (2016) 440–457.
[8] J.D. Madden, R.A. Cush, T.S. Kanigan, I.W. Hunter, Fast contracting polypyrrole actuators, Synth. Met. 113 (2000) 185–192.
[9] E. Smela, W. Lu, B.R. Mattes, Polyaniline actuators – part 1. PANI(AMPS) in HCl, Synth. Met. 151 (2005) 25–42.
[10] Y. Sonoda, W. Takashima, K. Kaneto, Characteristics of soft actuators based on polypyrrole films, Synth. Met. 119 (2001) 267–268.
[11] G.M. Spinks, L. Liu, G.G. Wallace, D.Z. Zhou, Strain response from polypyrrole actuators under load, Adv. Funct. Mater. 12 (2002) 437–440.
[12] S. Hara, T. Zama, W. Takashima, K. Kaneto, Artificial muscles based on polypyrrole actuators with large strain and stress induced electrically, Polym. J. 36 (2004) 151–161.
[13] G.G. Wallace, G.M. Spinks, L.A.P. Kane-Maguire, P.R. Teasdale, Conductive Electroactive Polymers: Intelligent Materials Systems, Second ed., CRC Press, Boca Raton, FL, USA, 2003.
[14] F.H. Meng, Y. Ding, Sub-micrometer-thick all-solid-state supercapacitors with high power and energy densities, Adv. Mater. 23 (2011) 4098–4102.
[15] X.Y. Lang, L. Zhang, T. Fujita, Y. Ding, M.W. Chen, Three-dimensional bicontinuous nanoporous Au/polyaniline hybrid films for high-performance electrochemical supercapacitors, J. Power Sources 197 (2012) 325–329.
[16] R. Li, K. Sieradzki, Ductile-Brittle transition in random porous Au, Phys. Rev. Lett. 68 (1992) 1168–1171.
[17] J. Erlebacher, M.J. Aziz, A. Karma, N. Dimitrov, K. Sieradzki, Evolution of nanoporosity in dealloying, Nature 410 (2001) 450–453.
[18] J. Weissmüller, R.C. Newman, H.J. Jin, A.M. Hodge, J.W. Kysar, Nanoporous metals by alloy corrosion: formation and mechanical properties, MRS Bull. 34 (2009) 577–586.
[19] J. Snyder, P. Asanithi, A.B. Dalton, J. Erlebacher, Stabilized nanoporous metals by dealloying ternary alloy precursors, Adv. Mater. 20 (2008) 4883–4886.
[20] H.J. Jin, S. Parida, D. Kramer, J. Weissmüller, Sign-inverted surface stress-charge response in nanoporous gold, Surf. Sci. Rep. 602 (2008) 3588–3594.
[21] H.J. Jin, X.L. Wang, S. Parida, K. Wang, M. Seo, J. Weissmüller, Nanoporous Au-Pt alloys As large strain electrochemical actuators, Nano Lett. 10 (2010) 187–194.
[22] C.A. Volkert, E.T. Lilleodden, Size effects in the deformation of sub-micron Au columns, Philos. Mag. 86 (2006) 5567.
[23] J. Biener, A.M. Hodge, J.R. Hayes, C.A. Volkert, L.A. Zepeda-Ruiz, A.V. Hamza, et al., Size effects on the mechanical behavior of nanoporous Au, Nano Lett. 6 (2006) 2379–2382.
[24] H.J. Jin, L. Kurmanaeva, J. Schmauch, H. Rosner, Y. Ivanisenko, J. Weissmüller, Deforming nanoporous metal: role of lattice coherency, Acta Mater. 57 (2009) 2665–2672.
[25] A. Mathur, J. Erlebacher, Size dependence of effective Young's modulus of nanoporous gold, Appl. Phys. Lett. 90 (2007).
[26] N. Mameka, K. Wang, J. Markmann, E.T. Lilleodden, J. Weissmüller, Nanoporous gold –Testing macro-scale samples to probe small-scale mechanical behavior, Mater Res Lett 4 (2016) 27–36.
[27] K. Wang, J. Weissmüller, Composites of nanoporous gold and polymer, Adv. Mater. 25 (2013) 1280–1284.
[28] K. Wang, A. Kobler, C. Kubel, H. Jelitto, G. Schneider, J. Weissmüller, Nanoporous-gold-based composites: toward tensile ductility, NPG Asia Mater. 7 (2015) e187.
[29] J. Weissmüller, R.N. Viswanath, D. Kramer, P. Zimmer, R. Würschum, H. Gleiter, Charge-induced reversible strain in a metal, Science 300 (2003) 312–315.
[30] J. Biener, A. Wittstock, L.A. Zepeda-Ruiz, M.M. Biener, V. Zielasek, D. Kramer, et al., Surface-chemistry-driven actuation in nanoporous gold, Nat. Mater. 8 (2009) 47–51.
[31] H.-J. Jin, J. Weissmüller, Bulk nanoporous metal for actuation, Adv. Eng. Mater. 12 (2010) 714–723.
[32] E. Detsi, M.S. Sellès, P.R. Onck, J.T.M. De Hosson, Nanoporous silver as electrochemical actuator, Scripta Mater. 69 (2013) 195–198.
[33] Q. Bai, Y. Wang, J. Zhang, Y. Ding, Z. Peng, Z. Zhang, Hierarchically nanoporous nickel-based actuators with giant reversible strain and ultrahigh work density, J. Mater. Chem. C 4 (2016) 45–52.
[34] J. Weissmüller, J.W. Cahn, Mean stresses in microstructures due to interface stresses: a generalization of a capillary equation for solids, Acta Mater. 45 (1997) 1899–1906.
[35] W. Haiss, Surface stress of clean and adsorbate-covered solids, Rep. Prog. Phys. 64 (2001) 591–648.
[36] D. Kramer, R.N. Viswanath, J. Weissmüller, Surface-stress induced macroscopic bending of nanoporous gold cantilevers, Nano Lett. 4 (2004) 793–796.
[37] R.N. Viswanath, D. Kramer, J. Weissmüller, Adsorbate effects on the surface stress-charge response of platinum electrodes, Electrochim. Acta 53 (2008) 2757–2767.
[38] J. Zhang, Q. Bai, Z. Zhang, Dealloying-driven nanoporous palladium with superior electrochemical actuation performance, Nanoscale 8 (2016) 7287–7295.
[39] X. Xiao, M.e. Wang, H. Li, P. Si, One-step fabrication of bio-functionalized nanoporous gold/poly(3, 4-ethylenedioxythiophene) hybrid electrodes for amperometric glucose sensing, Talanta 116 (2013) 1054–1059.
[40] E. Detsi, P. Onck, J.T.M. De Hosson, Metallic muscles at work: high rate actuation in nanoporous Gold/Polyaniline composites, Acs Nano 7 (2013) 4299–4306.
[41] B.Z. Yan, J. Yang, Y.F. Li, R.Y. Qian, Cyclic voltammetry of polypyrrole in anhydrous acetonitrile, Synth. Met. 58 (1993) 17–27.
[42] S. Shimoda, E. Smela, The effect of pH on polymerization and volume change in PPy(DBS), Electrochim. Acta 44 (1998) 219–238.
[43] J.B. Schlenoff, H. Xu, Evolution of physical and electrochemical properties of polypyrrole during extended oxidation, J. Electrochem. Soc. 139 (1992) 2397–2401.
[44] T. Osaka, T. Momma, S.-i. Komaba, H. Kanagawa, S. Nakamura, Electrochemical process of formation of an insulating polypyrrole film, J. Electroanal. Chem. 372 (1994) 201–207.
[45] T.W. Lewis, G.G. Wallace, C.Y. Kim, D.Y. Kim, Studies of the overoxidation of polypyrrole, Synth. Met. 84 (1997) 403–404.
[46] T. Shoa, J.D.W. Madden, T. Mirfakhrai, G. Alici, G.M. Spinks, G.G. Wallace, Electromechanical coupling in polypyrrole sensors and actuators, Sensor Actuat. A: Phys. 161 (2010) 127–133.
[47] C. Stenner, L.-H. Shao, N. Mameka, J. Weissmüller, Piezoelectric gold strong charge-load response in a metal-based hybrid nanomaterial, Adv. Funct. Mater. 26 (2016) 5174–5181.
[48] N. Mameka, J. Markmann, H.-J. Jin, J. Weissmüller, Electrical stiffness modulation – confirming the impact of surface excess elasticity on the mechanics of nanomaterials, Acta Mater. 76 (2014) 272–280.
[49] F. Weigend, F. Evers, J. Weissmüller, Structural relaxation in charged metal surfaces and cluster ions, Small 2 (2006) 1497–1503.
[50] J.M. Albina, C. Elsässer, J. Weissmüller, P. Gumbsch, Y. Umeno, Ab initio investigation of surface stress response to charging of transition and noble metals, Phys. Rev. Bk 85 (2012) 125118.
[51] K. Kaneto, Y. Sonoda, W. Takashima, Direct measurement and mechanism of electro-chemomechanical expansion and contraction in polypyrrole films, Jpn. J. Appl. Phys. Part 1-Regul. Papers Short Notes Rev. Pap. 39 (2000) 5918–5922.
[52] N. Alizadeh, F. Tavoli, Enhancing electrochromic contrast and redox stability of nanostructure polypyrrole film doped by heparin as polyanion in different solvents, J. Polym. Sci. A Polym. Chem. 52 (2014) 3365–3371.
[53] J.G. Martinez, T.F. Otero, E.W. Jager, Effect of the electrolyte concentration and substrate on conducting polymer actuators, Langmuir 30 (2014) 3894–3904.
[54] J.G. Martinez, T.F. Otero, E.W. Jager, Electrochemo-dynamical characterization of polypyrrole actuators coated on gold electrodes, Phys. Chem. Chem. Phys. 18 (2016) 827.
[55] L. Bay, K. West, P. Sommer-Larsen, S. Skaarup, M. Benslimane, A conducting polymer artificial muscle with 12% linear strain, Adv. Mater. 15 (2003) 310–313.
[56] G.M. Spinks, G.G. Wallace, L. Liu, D. Zhou, Conducting polymers electromechanical actuators and strain sensors, Macromol. Symp. 192 (2003) 161–170.
[57] P. Murray, G.M. Spinks, G.G. Wallace, R.P. Burford, Electrochemical induced ductile—brittle transition in tosylate-doped (pTS) polypyrrole, Synth. Met. 97 (1998) 117–121.

Biographies

Ke Wang received PhD degree in materials physics and technology at Hamburg University of Technology (TUHH), Germany in 2015. Then, she continued her scientific work as a postdoctoral fellow at TUHH. Her current research interest is focus on the synthesis of novel nanoporous metal-polymer hybrid and in the development of electrochemical actuators.

Charlotte Stenner was born in Munich, Germany. She received the B.Sc. and M.Sc. in physics from Hamburg University, Germany in 2010 and in 2013. Currently, she is completing a Ph.D. in materials science with the research topic of nanoporous-gold based hybrid materials as sensors in Hamburg University of Technology, Germany.

Jörg Weißmüller graduated as Diplom-Ingenieur in Materials Science after studies at the Universität des Saarlandes and the University of Dundee. He received his Doctorate in Engineering from Universität des Saarlandes based on studies on metallic nanoglasses and later obtained the Venia Legendi in Experimental Physics from the same institution. Weissmüller has worked as a staff scientist at Institute für Neue Materialien in Saarbrücken, as a guest scientist at the National Institute of Standards and Technology in Gaithersburg and at the University of Wisconsin in Madison, and as a group leader at the Karlsruher Institut für Technologie's Institut für Nanomaterialien. He is now a full professor and head of the Institut für Werkstoffphysik und Werkstofftechnologie at Technische Universität Hamburg as well as the leader of the Hybride Materialsysteme group at Helmholtz-Zentrum Geesthacht. Weissmüller has been awarded the PROCOPE Fellowship by Deutscher Akademischer Austauschdienst, the Feodor Lynen-Fellowship by Alexander von Humboldt-Stiftung, and the Heisenberg-Fellowship by Deutsche Forschungsgemeinschaft. A highlight of his research contributions are his combined experimental and theory investigations of the mechanics of interfaces in materials microstructures and of the coupling between mechanics and chemistry at interfaces. Current research also includes nanoporous metals by dealloying as a model system for interface effects on plasticity, elasticity and function of nanomaterials.